Computational Materials Science 164 (2019) 166–170

Contents lists available at ScienceDirect

Computational Materials Science

journal homepage: www.elsevier.com/locate/commatsci

Electric field tunable electronic properties of P-ZnO and SiC-ZnO van der Waals heterostructures

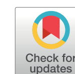

H.U. Din[a], M. Idrees[a], Tahani A. Alrebdi[b], Chuong V. Nguyen[c], B. Amin[a,*]

[a] Department of Physics, Hazara University, Mansehra 21300, Pakistan
[b] Department of Physics, Princess Nourah Bint Abdulrahman University, Riyadh, Saudi Arabia
[c] Department of Materials Science and Engineering, Le Quy Don Technical University, Hanoi 100000, Vietnam

ARTICLE INFO

Keywords:
2D-materials
vdW heterostructure
Electric-field
Type-II
DFT

ABSTRACT

The vertical stacking and influence of external electric field are good techniques to tune the electronic properties of two-dimensional materials for potential nanoelectronics and optoelectronic devices. The structural and electronic properties of P-ZnO and SiC-ZnO van der Waals (vdW) heterostructures are investigated by first principles calculations. P-ZnO (SiC-ZnO) heterostructure exhibits an indirect type-I (direct type-II) semiconducting band character. The effect of perpendicular applied external electric field on the electronic properties of the most stable vdW heterostructure has also been systematically discussed. Remarkable variations in the band gap nature are induced by increasing field strength from 0.1 to 1.0 V/Å (for P-ZnO) and 0.1 to 0.8 V/Å (for SiC-ZnO). The intrinsic indirect type-I is modulated to type-II semiconducting band gap in P-ZnO by applying electric field strength 0.1 V/Å. More interestingly, reduction in the size with transition from an indirect-to-direct type-II semiconductor band gap nature is noted at 0.5 V/Å. However, a direct type-II semiconductor to metallic character is found at 1.0 V/Å (for P-ZnO) and 0.8 V/Å (for SiC-ZnO). Our results suggests that these vdW heterostructures are promising candidates for electronic and optoelectronic device applications.

1. Introduction

In recent years, beyond the successful growth of gapless graphene, two-dimensional (2D) materials have been greatly focused in research community due to their distinctive and tunable electronic properties in nanotechnology and optoelectronics [1–4]. A large number of 2D materials including hexagonal Boron Nitride (h-BN) [5,6], transition metal dichalcogenides (TMDs) [5], blue phosphorene (P) [7,8], SiC [9,10] and ZnO [11] have drawn extensive attention because of the novel photovoltaic and optoelectronic properties in contrast to their bulk counterparts [5].

Meanwhile, ZnO exhibits the graphene-like unique 2D-planar honeycomb structure with sp^2-bonding between Zn and O atoms, is gaining a great attention in nanotechnology [11]. The fascinating chemical bonding of low dimensional ZnO leads to emerging applications in transparent electronics, solar cells, gas sensors, and biomedical devices [12]. Analogous to ZnO monolayer, SiC monolayer is also reported as a dynamically more stable in planar geometry than low buckled or zigzag phases [10,13]. Single layer SiC possesses intriguing electronic properties with nonmagnetic semiconducting band gap offering high carrier mobility, large in-plane stiffness and strong thermostability [8,9,13-15]. Blue phosphorene (P), another promising 2D semiconducting material, has been extensively focused owing to its extraordinary properties including ultra-high mobility and sizable band gap [8,16]. Single layer blue P has been potentially addressed as a promising candidate for thermoelectric material and superconductivity [17,18].

Recently, stacking of monolayers via van der Waals (vdW) interaction has been found as an emerging technique to overcome the restricted properties of single material systems and constructing heterostructures with more enviable physical properties for development and various optoelectronic applications [19]. For instance, SiC/TMDs are theoretically reported as promising for optoelectronic and photocatalytic water splitting [20], MoS_2/Si is useful in solar cell applications [21], BlueP/graphene and BlueP/g-GaN heterostructures are effective for carrier dynamics and new electronic devices [22] and TMDs/ZnO are suitable for optical devices [23]. Further, band gap engineering by applying external electric field is also an important strategy to modulate the electronic properties for realizing significant optical and optoelectronic applications. In particular, tuning the electronic band gap from indirect to direct under external electric field is essential for designing new high performance optoelectronic devices. It has been demonstrated both experimentally and theoretically that the effective control of band structure of bilayer-MoS_2 and further semiconductor-to-metal transition is realized under electric field [24]. Transition from type-I to type-II in

* Corresponding author.

https://doi.org/10.1016/j.commatsci.2019.04.016
Received 18 February 2019; Received in revised form 7 April 2019; Accepted 10 April 2019
0927-0256/ © 2019 Published by Elsevier B.V.

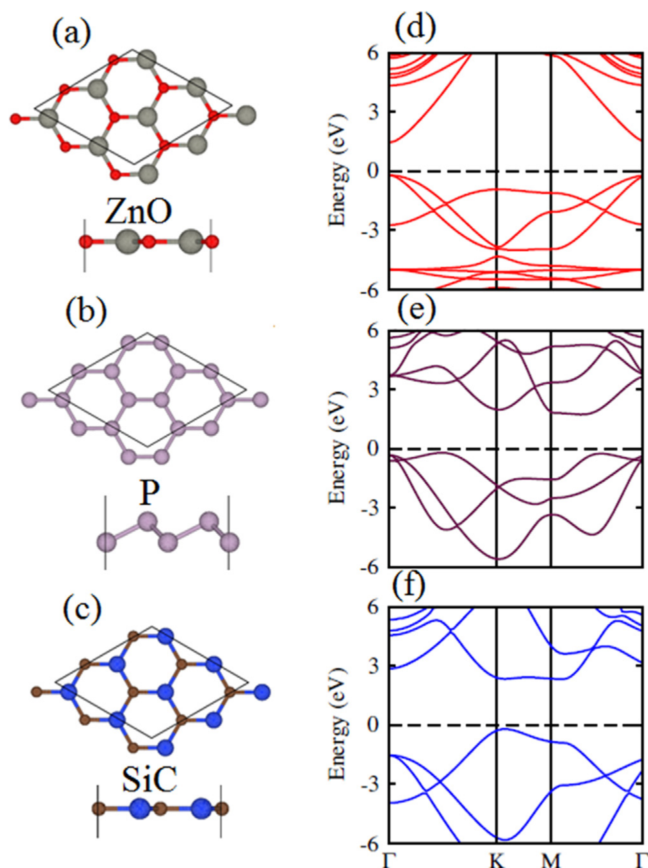

Fig. 1. Top and side view (a–c), the electronic band structures (d–f) using PBE-functional of ZnO, blue phosphorene and SiC monolayers, respectively.

ZrS_2/HfS_2 and $MoSe_2/MoS_2$ and $CrSe_2/MoS_2$ has been achieved by applying an electric field [3,25]. M. Sun et al. reported dynamic switching between n-type and p-type Schottky contacts in BlueP/graphene under perpendicular electric field, which is important for novel Schottky devices [22]. This indicates that the role of vdW heterostructures and applied external electric field is crucial for designing novel optoelectronic devices based on 2D materials.

The dynamical stability and same hexagonal crystal structure of single layer blue phosphorene (P) and SiC realize the fact to construct appropriate vdW heterostructures with ZnO monolayer. It is further worth noting that the lattice constants of P and SiC perfectly match with ZnO hence; anticipate to explore the electronic properties of these vdW heterostructures for versatile optoelectronic properties. In the study reported here, the structural and electronic properties of P-ZnO and SiC-ZnO vdW heterostructures are performed by first-principles calculations. More interestingly, the external electric field applied perpendicular to these vdW heterostructures has dramatically modified the electronic properties with indirect to direct band gap semiconducting transition for P-ZnO and further reduction from semiconducting to metal transition in both under study systems.

Table 1
Lattice constant (Å), binding energy (E_i, E_{ii}, E_{iii}, E_{iv}, E_v, E_{vi}, in eV), interlayer distance ($d_{spacing}$, in Å), bond-length (Å), and band gap ($E_{g\text{-PBE}}$, in eV) for P-ZnO and SiC-ZnO heterostructures.

Parameters	P-ZnO	SiC-ZnO
a (Å)	3.29	3.20
E_i (eV)	−0.17	−0.42
$d_{spacing}$	3.72	3.53
E_{ii} (eV)	−0.30	−0.93
$d_{spacing}$	3.39	2.79
E_{iii} (eV)	−0.26	−0.92
$d_{spacing}$	3.48	2.93
E_{iv} (eV)	–	−0.85
$d_{spacing}$		2.95
E_v (eV)	–	−0.41
$d_{spacing}$		3.01
E_{vi} (eV)	–	−0.91
$d_{spacing}$		2.86
P-P/Zn-O (Å)	2.26/1.89	–
Si-C/Zn-O (Å)	–	1.847/1.848
$E_{g\text{-PBE}}$ (eV)	1.275	2.27

1.1. Computational details

First principles calculations based on density functional theory (DFT) [26] with projector augmented wave (PAW) scheme [27] are performed using Vienna ab-initio Simulation Package (VASP) [28] within the projector augmented wave method. The generalized gradient approximation (GGA) with the Perdew-Burke-Ernzerhof (PBE) functional [29] is adopted to demonstrate the exchange-correlation functional. The vdW interactions in the heterostructures are described by taking in to account the empirical dispersioncorrection using the Grimme (DFT (PBE)-D2) method [30]. Additionally, the Heyd–Scuseria–Ernzerhof (HSE06) hybrid functional [31] is also adopted for electronic band structure calculations. A $6 \times 6 \times 1$ Γ-centered Monkhorst–Pack k-mesh is used for geometric optimization using GGA-PBE-functional and $12 \times 12 \times 1$ k-mesh is chosen for electronic structure calculations (using both PBE and HSE06 functional). All the atoms are fully relaxed until the forces and energy have converged to −0.01 eV/Å and 10^{-4} eV, respectively. A plane wave cut-off energy of 500 eV is used for these calculations. A vacuum layer of 30 Å is added to eliminate interactions between adjacent images in these systems. In addition, the external electric field, applied normal to the plane of the

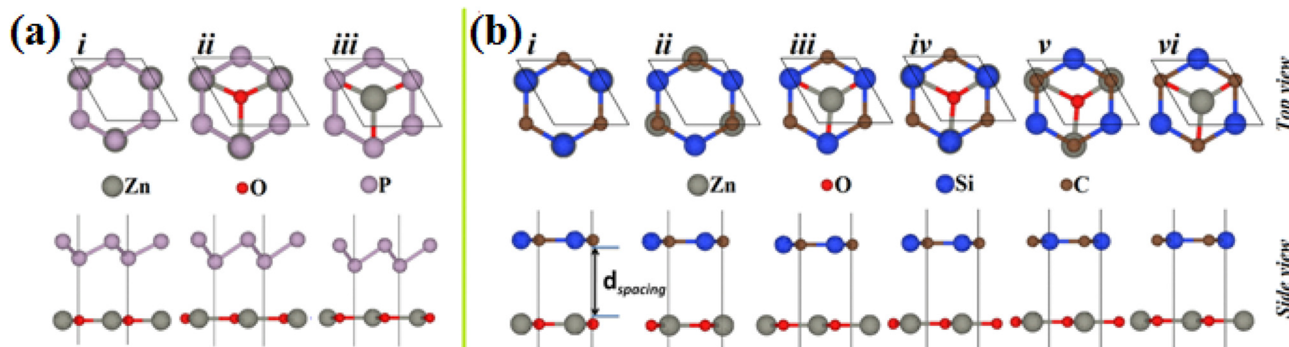

Fig. 2. Top and side view of; (a) P-ZnO heterostructure (i–iii) and (b) SiC-ZnO heterostructure (i–vi) with possible stacking configurations, see text for details.

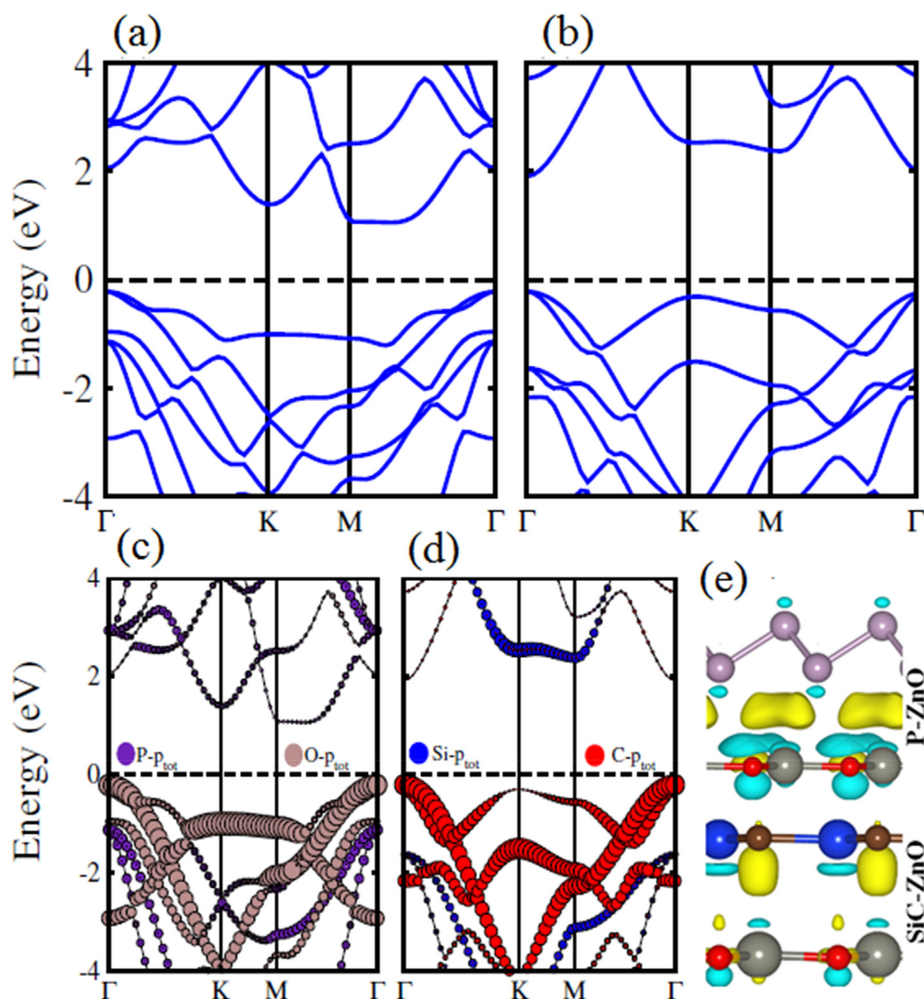

Fig. 3. Electronic band structures (a, b), weighted band structures (c, d) and charge density difference with isovalue 0.0015 e/Å^3 (e), of P-ZnO and SiC-ZnO heterostructures, respectively.

heterostructures, is taken in to account by adding dipole correction (with DIPOL = 0.5 0.5 0.5) in the unit cell. Initially, the band gap is nonlinear with zero slope to the applied electric field (E = 0 V/Å). For larger fields, the response of band gap is linear and the slope of the curve can be written as

$$\frac{dE_g}{dE} = -eS \tag{1}$$

where e and Srepresent the electron charge and the giant Stark effect respectively. According to Zheng et al., since the potential of the external electric field is $eE\,z$, the change in the band gap due to applied electric field is approximately

$$\Delta E_g = eE\langle z\rangle_{cb} - eE\langle z\rangle_{vb} \tag{2}$$

where $\langle z\rangle_{cb}$ and $\langle z\rangle_{vb}$ denote the centre of the conduction and valence band along the direction of the applied electric field, respectively [32].

2. Results & discussion

Single layer blue P and ZnO/SiC exhibit buckled and planar crystal symmetry with unit cell as depicted in Fig. 1(a–c), respectively. The optimized lattice constant (bond-length) 3.28 (1.90), 3.27 (2.25) and 3.10 (1.79) Å for ZnO, P and SiC monolayers respectively, are in good agreement with available literature [7–13]. Small lattice mismatch for P-ZnO (0.3%) and SiC-ZnO (5.48%) is crucial for designing novel heterostructures. Different possible stacking configurations based on the optimized lattice constants of ZnO, P and SiC monolayers are studied, see Fig. 2. For P-ZnO heterostructure (see Fig. 2a) with; (i) Each P-atom is located on both Zn and O-atoms, (ii) P-atom is lying on the top of Zn-atom and O-atom is fixed at hexagonal centre (iii) P-atom is placed on the top of O-atom and Zn-atom is located at hollow site while for SiC-ZnO heterostructure (see Fig. 2b) where; (i) Si(C)-atom is sit on Zn(O)-atom, (ii) Si(C) is lying on the top of O(Zn)-atom, (iii) Si-atom is sit on the top position of the O-atom and Zn-atom is fixed on hollow site, (iv) Si-atom is directly positioned on the top of Zn-atom with O-atom is lying on hollow site, (v) C(O)-atom is placed on the top of Zn (hollow) position, and (vi) C(Zn)-atom is positioned on the top of O(hollow)-site. The binding energy (E) defined as: $E = E_{Hetero} - E_{ZnO} - E_{P/SiC}$, where E_{Hetero}, E_{ZnO} and $E_{P/SiC}$ represent the total energy of heterobilayer, ZnO and P/SiC monolayer systems, respectively. The calculated binding energy (E) and interlayer distance ($d_{spacing}$) of all stacking are listed in Table 1. One can obviously note that both heterobilayers favors type-ii stacking due to smaller $d_{spacing}$ and greater binding energy than other configurations. Moreover, the formation of both interfaces is exothermic due to negative binding energy. The optimized lattice constants and bond-length, presented in Table 1, indicate that lattice mismatch induces an intrinsic compressive (tensile) strain in ZnO (P and SiC) monolayers of the understudy heterobilayer systems as compared to their corresponding freestanding monolayers [20,22,23].

A comprehensive insight is gained into the electronic properties by performing the electronic band structure calculations of both heterostructures and their corresponding monolayers. First, we present the band structures of 2D monolayers of ZnO, P and SiC (see Fig. 1(c–e)

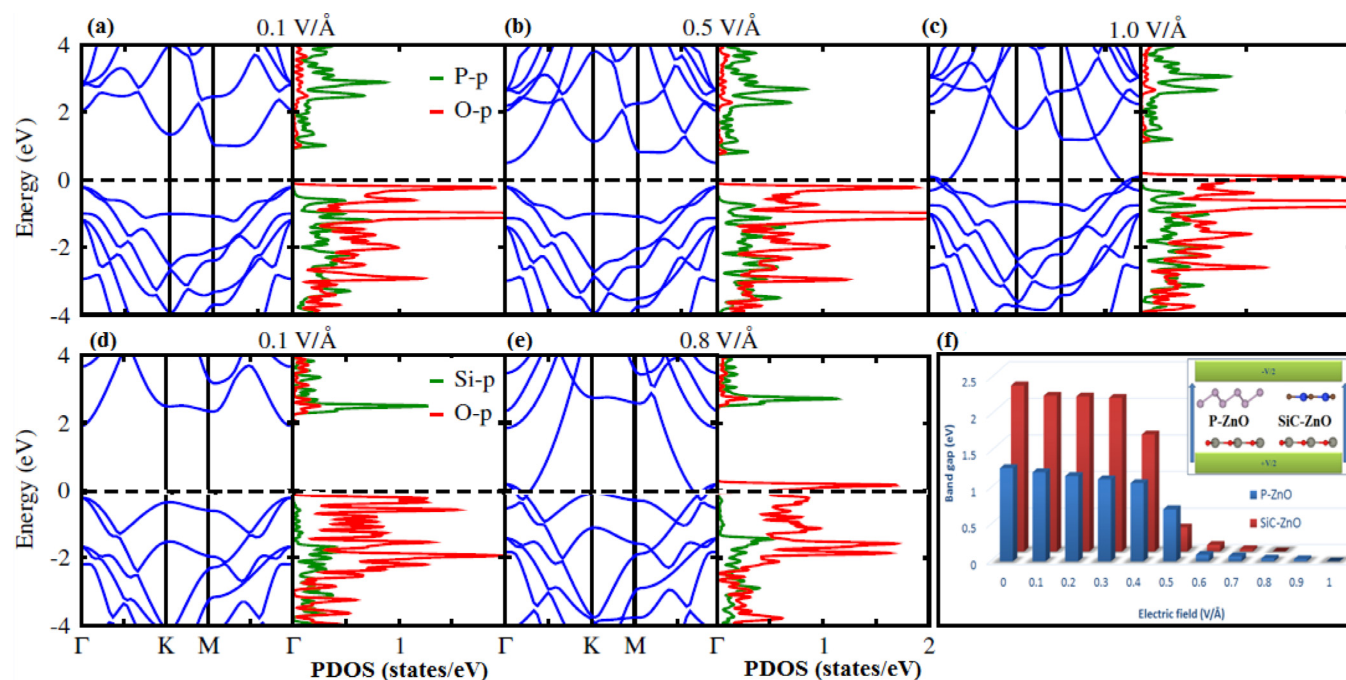

Fig. 4. Electronic band structure and partial density of states (PDOS) under external electric field of strength: (a) 0.1 V/Å , (b) 0.5 V/Å, (c) 1.0 V/Å for P-ZnO, (d) 0.1 V/Å, (e) 0.8 V/Å for SiC-ZnO, and (f) band gap values versus external electric, where the red and blue bars represent the P-ZnO and SiC-Zno heterostructures, respectively and the direction of external electric field is shown in the inset.

respectively) using PBE functional to ensure the accuracy of our results. Additionally, HSE06 is adopted to study the electronic properties of these monolayers. The conduction band minimum (CBM) and the valence band maximum (VBM) located; both at Γ-point (for ZnO), at about the middle of M-Γ-point (for blue P), and M- and Γ-point (for SiC) respectively, presenting direct (indirect) band gap nature for ZnO and P (SiC) with values 1.65 (3.13), 1.95 (2.87) and 2.43 (3.23) eV using PBE (HSE06) respectively. These results are consistent with available literature [7–13,16], indicating the reliability of methods adopted for these calculations. From calculated partial density of states (PDOS), it is noted that both VBM and CBM near the Fermi level (E_F) are mainly contributed by O-2p_z(P-3p_z) state of ZnO(P) monolayer whereas C-2p_z majorly dominates the VBM and CBM is due to Si-3p_z state of SiC monolayer.

In DFT, HSE06 functional presents better agreement with experiments in comparison to PBE functional. However, this trend is not generalized and depends upon the material under study [33]. It has been reported that PBE (HSE06) functional underestimates (overestimates) the experimental band gap value by 0.12 (0.45) eV in MoS_2 monolayer [33–36]. Lack of available experimental results and qualitative consistent characteristics of HSE06 and PBE band structures, realize us to rely on PBE calculations for the electronic behavior of the understudy heterobilayer system.

Now we turn our focus to the calculated band structures of P-ZnO and SiC-ZnO heterostructures, as listed in Table 1 and visualized in Fig. 3(a, b). For P-ZnO heterostructure, the VBM and CBM lyingabout at the middle of M-Γ- and Γ-point indicate indirect band nature using PBE method. However, SiC-ZnO possesses the characteristics of direct band gap with VBM and CBM both lying at Γ-point of the Brillouin zone. Further, a careful observation of the band structures, see in Figs. 1(d–f) and 3(a, b), shows that CBM and VBM positions are localized in blue P (for P-ZnO), and SiC and ZnO (for SiC-ZnO) monolayers and resulting in type-I and type-II band alignment respectively, which is crucial for optoelectronic applications [37].

To shed further light on the localized orbital reconfiguration, we plot the orbital weighted band structures of P-ZnO and SiC-ZnO heterostructures in Fig. 3(c, d). Obviously, P-3p (P) is dominant in both CBM and VBM for P-ZnO, indicating type-I band alignment (straddling gap). However, the CBM is mainly contributed by C-2p (SiC) states and VBM is dominated by O-2p (ZnO) state in SiC-ZnO heterostructures. Hence, VBM and CBM localized in different constituent layers of SiC-ZnO heterostructure, are termed as type-II band alignment (staggered gap). Although type-II band alignment is achieved in homogenous bilayers under external electric field [36]. However, type-II band alignment achieved in SiC-ZnO heterostructures in the absence of electric field making it prominent for potential applications in light detection and harvesting [20,23,37].

Additionally, the Bader charge population analysis [38,39] and charge density difference (Δρ), expressed as $\Delta\rho = \rho_{Hetero} - \rho_{ZnO} - \rho_{P/SiC}$, in order to understand the interaction between P/SiC and ZnO monolayers, where ρ_{Hetero}, $\rho_{P/Si}$ and ρ_{ZnO} denote the charge densities of heterostructures, P/SiC and ZnO monolayers, respectively. As shown in Fig. 3e, the cyan and yellow colors represent the charge depletion and accumulation, respectively. One can clearly observe that electrons are mainly depleted on the upper layer of Zn atom (in ZnO monolayer) and accumulated at the interlayer region for P (in P-ZnO) and at the C-atom of SiC monolayer (in SiC-ZnO). However, it is further ensured by Bader population analysis that the small amount of charge 0.0114|e| transferred from ZnO to SiC monolayer, result in built-in electric field and responsible for type-II band alignment. This small amount of charge transfer also indicates weak vdW interaction between monolayers in SiC-ZnO heterostructures which has also been reported in Refs. [13,40]. Additionally, majority of charge is driven from ZnO to P (in P-ZnO) and SiC (in SiC-ZnO), making it p-type semiconductor after vdW stacking with P and SiC monolayers, respectively.

In general, the heterostructures used in the electronic and photoelectronic devices, are subjected to experience external electric field. Thus, it is important to explore the electronic properties of P-ZnO and SiC-ZnO heterostructures under external electric field along z-direction, see inset in Fig. 4f. Since, electric field applied in negative direction only enlarges the band gap with no considerable alteration in the type of band alignment therefore; external electric field in the positive direction is mainly taken into account here. In Fig. 4(a–e), the electronic band structures and partial density of states (PDOS) of these

heterobilayers are presented with different strengths of electric fields. The positive direction electric field is taken from ZnO to P(SiC) monolayer. For P-ZnO heterostructure, a small decrease in band gap is noted with increase in strength of electric field from 0.1 to 0.4 V/Å. A dramatic transition from type-I to type-II band alignment (with VBM (CBM) dominated by p-states of O(P) atoms in P-ZnO) is found under the external electric field strength (0.1–0.9 V/Å). More interestingly, an indirect (type-II) to direct (type-II) semiconducting band gap transition with VBM and CBM (shifted down) located at Γ-point of the Brillouin zone, is noted at 0.5 V/Å electric field strength, see Fig. 4b, and this direct band gap character (with decreasing value) is preserved under 0.6–0.9 V/Å, see in Fig. 4f. However, a direct semiconducting band gap to metal transition is observed with further increasing the electric field to 1.0 V/Å, see Fig. 4c. Similar tendencies in reduction in band gap from direct type-II semiconducting gap to metal transition is also demonstrated in SiC-ZnO under 0.1–0.8 V/Å electric field strength, see Fig. 4(d, e). Moreover, it is clear from calculated partial density of states (PDOS) that P-3p/Si-3p and O-2p states hybridize at Fermi level in P-ZnO/SiC-ZnO heterobilayer systems as shown in Fig. 4(c, e). These drastic variation in the type and size of band gap are attributed to the orbitals located at Γ-point of CBM, which are highly sensitive to the applied perpendicular electric field than orbitals of the M-point of VBM [41].

3. Conclusion

To summarize, first principles calculations are performed to investigate and modulate the electronic properties of P-ZnO and SiC-ZnO vdW heterostructures under the perpendicular external electric filed. The commensurate heterostructures reveal indirect type-I (direct type-II) semiconducting band character in P-ZnO (SiC-ZnO). A dramatic transition from type-I to type-II semiconducting band alignment occurs in P-ZnO under the external electric field strength 0.1 V/Å. Interestingly, an indirect to direct type-II semiconducting band transition with reduced band gap value is found when the applied field reaches 0.5 V/Å. Furthermore, increase in electric field drastically reduces the size of band gap of P-ZnO (from 0.1 to 0.9 V/Å) and SiC-ZnO (from 0.1 to 07 V/Å). However, a direct type-II semiconductor to metallic nature is obtained at 1.0 V/Å (for P-ZnO) and 0.8 V/Å (for SiC-ZnO). The present work is beneficial and opens up an avenue for potential applications of these heterostructures in electronic and optoelectronic device applications.

Acknowledgements

Higher Education Commission of Pakistan (Grant No. 5727/KPK/NRPU/R&D/HEC2016) and the Vietnam National Foundation for Science and Technology Development (NAFOSTED) (Grant No. 103.01-2016.07) and Deanship of Scientific Research. Princess Nourah Bint Abdulrahman University, Riyadh. Saudi Arabia are gratefully acknowledged.

References

[1] Q.H. Wang, K.K. Zadeh, A. Kis, J.N. Coleman, M.S. Strano, Electronics and optoelectronics of two-dimensional transition metal dichalcogenides, Nat. Nanotechnol. 7 (2012) 699.
[2] C.X. Xia, J. Li, Recent advances in optoelectronic properties and applications of two-dimensional metal chalcogenides, J. Semicond. 37 (2016) 051001.
[3] J. Shang, S. Zhang, X. Cheng, Z. Wei, J. Li, Electric field induced electronic properties modification of ZrS_2/HfS_2 van der Waals heterostructure, RSC Adv. 7 (2017) 14625.
[4] K.S. Novoselov, A.K. Geim, S.V. Morozov, D. Jiang, Y. Zhang, S.V. Dubonos, I.V. Grigorieva, A.A. Firsov, Electric field effect in atomically thin carbon films, Science 306 (2004) 666.
[5] J.N. Coleman, M. Lotya, A. O'Neill, S.D. Bergin, P.J. King, U. Khan, K. Young, A. Gaucher, S. De, R.J. Smith, I.V. Shvets, S.K. Arora, G. Stanton, H.-Y. Kim, K. Lee, G.T. Kim, G.S. Duesberg, T. Hallam, J.J. Boland, J.J. Wang, J.F. Donegan, J.C. Grunlan, G. Moriarty, A. Shmeliov, R.J. Nicholls, J.M. Perkins, E.M. Grieveson, K. Theuwissen, D.W. McComb, P.D. Nellist, V. Nicolosi, Two-dimensional nanosheets produced by liquid exfoliation of layered materials, Science 331 (2011) 568.
[6] H. Dang, Y. Liu, W. Xue, R.S. Anderson, C.R. Sewell, S. Xue, D.W. Crunkleton, Y. Shen, S. Wang, Phase transformations of nano-sized cubic boron nitride to white graphene and white graphite, Appl. Phys. Lett. 104 (2014) 093104.
[7] L. Li, Y. Yu, G.J. Ye, Q. Ge, X. Ou, H. Wu, D. Feng, X.H. Chen, Y. Zhang, Black phosphorus field-effect transistors, Nat. Nanotechnol. 9 (2014) 372.
[8] Z. Zhu, D. Tomanek, Semiconducting layered blue phosphorus: a computational study, Phys. Rev. Lett. 112 (2014) 176802.
[9] L. Sun, Y. Li, Z. Li, Q. Li, Z. Zhou, Z. Chen, J. Yang, J.G. Hou, Electronic structures of SiC nanoribbons, J. Chem. Phys. 129 (2008) 174114.
[10] H. Şahin, S. Cahangirov, M. Topsakal, E. Bekaroglu, E. Akturk, R.T. Senger, S. Ciraci, Monolayer honeycomb structures of group-IV elements and III-V binary compounds: first-principles calculations, Phys. Rev. B 80 (2009) 155453.
[11] M. Topsakal, S. Cahangirov, E. Bekaroglu, S. Ciraci, First-principles study of zinc oxide honeycomb structures, Phys. Rev. B 80 (2009) 235119.
[12] Q. Tang, Y. Li, Z. Zhou, Y. Chen, Z. Chen, Tuning electronic and magnetic properties of wurtzite ZnO nanosheets by surface hydrogenation, ACS Appl. Mater. Interfaces 2 (2010) 2442.
[13] E. Bekaroglu, M. Topsakal, S. Cahangirov, S. Ciraci, First-principles study of defects and adatoms in silicon carbide honeycomb structures, Phys. Rev. B 81 (2010) 075433.
[14] S.S. Lin, Light-emitting two-dimensional ultrathin silicon carbide, J. Phys. Chem. C 116 (2012) 3951.
[15] K.X. Zhu, L.W. Guo, J.J. Lin, W.C. Hao, J. Shang, Y.P. Jia, L.L. Chen, S.F. Jin, W.J. Wang, X.L. Chen, Graphene covered SiC powder as advanced photocatalytic material, Appl. Phys. Lett. 100 (2012) 023113.
[16] J. Xiao, M. Long, X. Zhang, J. Ouyang, H. Xu, Y. Gao, Theoretical predictions on the electronic structure and charge carrier mobility in 2D phosphorus sheets, Sci. Rep. 5 (2015) 09961.
[17] C. Sevik, H. Sevinçli, Promising thermoelectric properties of phosphorenes, Nanotechnology 27 (2016) 355705.
[18] J.J. Zhang, S. Dong, Prediction of above 20 K superconductivity of blue phosphorus bilayer with metal intercalations, 2D Mater 3 (2016) 035006.
[19] B. Amin, N. Singh, U. Schwingenschlogl, Heterostructures of transition metal dichalcogenides, Phys. Rev. B 92 (2015) 075439.
[20] H.U. Din, M. Idrees, G. Rehman, C.V. Nguyen, L.-Y. Gan, I. Ahmad, M. Maqbool, B. Amin, Electronic structure, optical and photocatalytic performance of SiC–MX_2 (M = Mo, W and X = S, Se) van der Waals heterostructures, Phys. Chem. Chem. Phys. 20 (2018) 24168.
[21] M.L. Tsai, S.H. Su, J.K. Chang, D.S. Tsai, C.H. Chen, C.I. Wu, L.J. Li, L.J. Chen, J.H. He, Monolayer MoS_2 heterojunction solar cells, ACS Nano 8 (2014) 8317.
[22] M. Sun, J.P. Chou, J. Yu, W.C. Tang, Electronic properties of blue phosphorene/graphene and blue phosphorene/graphene-like gallium nitride heterostructures, Phys. Chem. Chem. Phys. 19 (2017) 17324.
[23] S. Wang, H. Tian, C. Ren, J. Yu, M. Sun, Electronic and optical properties of heterostructures based on transition metal dichalcogenides and graphene-like zinc oxide, Sci. Rep. 8 (2018) 12009.
[24] Q. Liu, L. Li, Y. Li, Z. Gao, Z. Chen, J. Lu, Tuning electronic structure of bilayer MoS_2 by vertical electric field: a first-principles investigation, J. Phy. Chem. C 116 (2012) 21556.
[25] N. Lu, H. Guo, L. Li, J. Dai, L. Wang, W.-N. Mei, X. Wu, X.C. Zeng, MoS_2/MX_2 heterobilayers: bandgap engineering via tensile strain or external electrical field, Nanoscale 6 (2014) 2879.
[26] W. Kohn, L.J. Sham, Self-consistent equations including exchange and correlation effects, Phys. Rev. 140 (1965) A1133.
[27] P.E. Blochl, Projector augmented-wave method, Phys. Rev. B 50 (1994) 17953.
[28] G. Kresse, J. Furthmüller, Efficient iterative schemes for ab initio total-energy calculations using a plane-wave basis set, Phys. Rev. B 54 (1996) 11169.
[29] J.P. Perdew, K. Burke, M. Ernzerhof, Generalized gradient approximation made simple, Phys. Rev. Lett. 77 (1996) 3865.
[30] S. Grimme, Semiempirical GGA-type density functional constructed with a long-range dispersion correction, J. Comput. Chem. 27 (2006) 1787.
[31] J. Heyd, G.E. Scuseria, M. Ernzerhof, Erratum: "Hybrid functionals based on a screened Coulomb potential", J. Chem. Phys. 124 (2006) 219906.
[32] F. Zheng, Z. Liu, J. Wu, W. Duan, B.-L. Gu, Scaling law of the giant Stark effect in boron nitride nanoribbons and nanotubes, Phys. Rev. B 78 (2008) 085423.
[33] P. Johari, V.B. Shenoy, Tuning the electronic properties of semiconducting transition metal dichalcogenides by applying mechanical strains, ACS Nano 6 (2012) 5449.
[34] K.F. Mak, C. Lee, J. Hone, J. Shan, T.F. Heinz, Atomically thin MoS_2: a new direct-gap semiconductor, Phys. Rev. Lett. 105 (2010) 136805.
[35] A. Kuc, N. Zibouche, T. Heine, Influence of quantum confinement on the electronic structure of the transition metal sulfide TS_2, Phys. Rev. B 83 (2011) 245213.
[36] C. Ataca, S. Ciraci, Functionalization of single-layer MoS_2 honeycomb structures, J. Phys. Chem. C 115 (2011) 13303.
[37] H.-P. Komsa, A.V. Krasheninnikov, Electronic structures and optical properties of realistic transition metal dichalcogenide heterostructures from first principles, Phys. Rev. B 88 (2013) 085318.
[38] R.F.W. Bader, Atoms in Molecules – A Quantum Theory, Oxford University Press, Oxford, 1990.
[39] G. Wang, A.K.F. Rahman, B. Wang, Ab initio calculations of ionic hydrocarbon compounds with heptacoordinate carbon, J. Mol. Model. 24 (2018) 116.
[40] Z. Huang, C. He, X. Qi, H. Yang, W. Liu, X. Wei, X. Peng, J. Zhong, Band structure engineering of monolayer MoS_2 on h-BN: first-principles calculations, J. Phys. D: Appl. Phys. 47 (2014) 075301.
[41] Y. Lee, Y. Hwang, S.B. Cho, Y.-C. Chung, Achieving a direct band gap in oxygen functionalized-monolayer scandium carbide by applying an electric field, Phys. Chem. Chem. Phys. 16 (2014) 26273.